

Supplementary Information

A highly sensitive label-free electrochemical immunosensing platform based on aligned GaN nanowires array/ polydopamine heterointerface modified with gold nanoparticles

Qingyun Liu,^a Taotao Yang,^a Yongqin Ye,^b Ping Chen,^a Xiaoning Ren,^a Ai Rao,^a Ying Wan,^a Bin Wang^{*b} and Zhiqiang Luo^{*a}

^a. College of Life Science and Technology, Huazhong University of Science and Technology, Wuhan 430074, China

^b. Department of General Surgery, Shenzhen Children's Hospital, Shenzhen 518026, China

* Corresponding Author, Email: zhiqiangluo@hust.edu.cn, szwb1967@126.com

Supplementary Figures and Notes

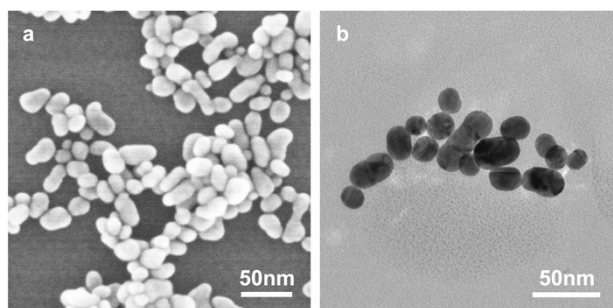


Figure S1 (a) SEM image and (b) TEM image of gold nanoparticles. From the images it could be seen that most of the nanorods are 20 nm nanoparticles.

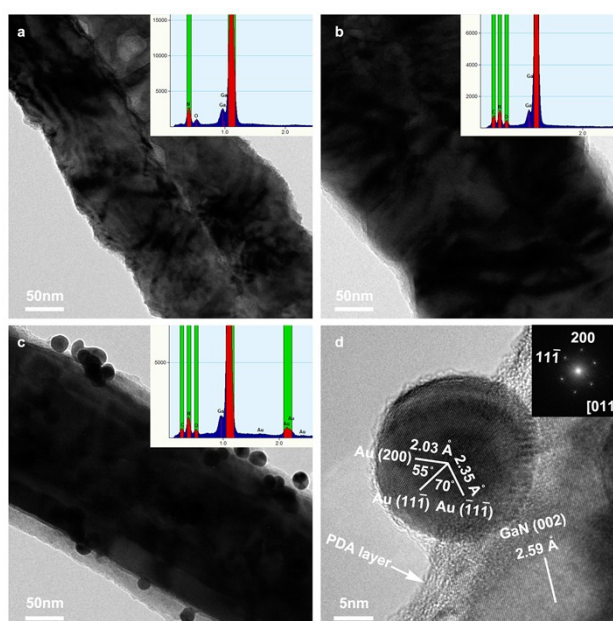


Figure S2 TEM images of (a) individual GaN nanowire, (b) GaN nanowire/PDA and (c) GaN nanowire/PDA/Au nanoparticles. Insets on top right are the corresponding EDS spectrum. Additional predominant C and O peaks are in the EDS spectrum of GaN nanowire/PDA samples, and an obvious Au peak is in the EDS spectrum of GaN nanowire/PDA/Au nanoparticles samples. (d) High-resolution TEM image of GaN nanowire/PDA/Au nanoparticles, inset corresponds to the selective area electron diffraction of the representative Au nanoparticle. The surface of single crystalline GaN nanowire is enclosed with a thin layer (5 nm) of PDA.

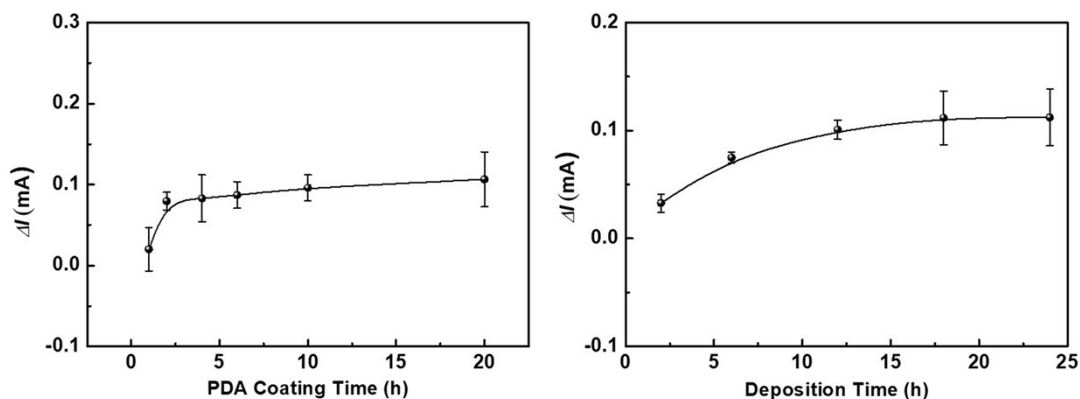


Figure S3 Effect of (a) PDA coating time and (b) Au nanoparticles deposition time on the electronic properties of GaN nanowires array.

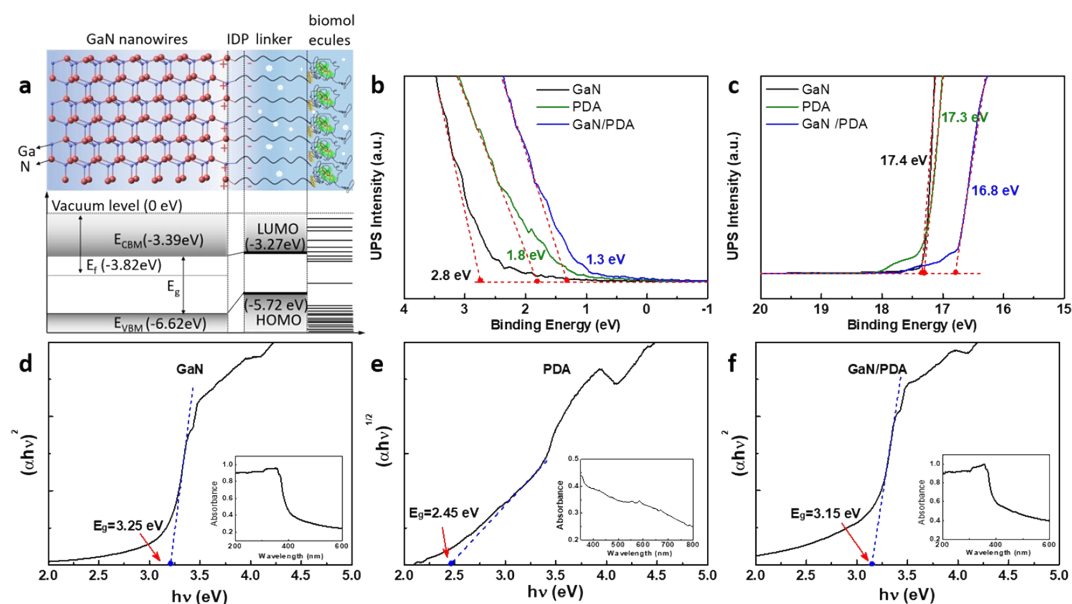


Figure S4 (a) Schematic diagram of the structural and electronic properties at the heterointerface in an idealized case; (Top) Biomolecules are covalently immobilized on the GaN nanowire surface via PDA as linker molecules. An interface dipole layer (IDP) is formed between GaN nanowire and PDA; (Bottom) Corresponding band diagram of GaN nanowire and PDA. On the GaN nanowire side, the electronic properties are depicted as conduction band maxima (E_{CBM}), Fermi-level (E_f) and valence band minima (E_{VBM}). On the PDA linker side, the electronic properties are described by highest occupied molecular orbital (HOMO) and lowest unoccupied molecular orbital (LUMO). It is worthy to be noticed that under most circumstances, the exact positions of energy levels will be affected by surface and interfacial properties. UPS spectra for (b) the onset energy and (c) the secondary cutoff of GaN (black curves), PDA (green curves) and GaN/PDA (blue curves); The Fermi levels are calibrated by an Au foil. The Tauc plots of (d) GaN, (e) PDA and (f) GaN/PDA; Insets show the corresponding UV-vis diffuse reflectance spectra.

Supplementary Notes: The energy levels of GaN and PDA are given in Figure S4a. The energy levels are determined combined UPS with UV-vis diffuse reflectance spectra. The valence band maxima (or

highest occupied molecular orbital, V_{VBM} or HOMO) and the conduction band minima (or lowest unoccupied molecular orbital, V_{CBM} or LUMO) can be calculated according to the following equations:¹⁻³

$$E_{VBM} = hv - E_{cutoff} - E_{onset} \quad (S1)$$

$$E_{CBM} = E_{VBM} - E_g \quad (S2)$$

where hv is the incident photon energy (21.22 eV) of He I, E_{cutoff} is the secondary cutoff edge, E_{onset} is the onset energy and E_g is the band gap. E_{onset} and E_{cutoff} are determined by extrapolating a straight line through the leading edge of the spectra (Figure S4b) and the yield of secondary electrons (Figure S4c) to zero, respectively. E_g are derived from the intercepts of the Tauc plots (Figure S4e-f), which are calculated according to the following equation:^{4, 5}

$$(ahv)^{1/n} = A(hv - E_g) \quad (S3)$$

where a is the absorption coefficient, h is the Planck's constant, A is the proportionality constant, exponent $n=1/2$ for direct bandgap semiconductors and $n=2$ for indirect bandgap semiconductors.

The calculated results of GaN, PDA and GaN/PDA are as follows: E_{VBM} (or HOMO) = -6.62 eV, -5.72 eV, -5.72 eV and E_g = 3.25 eV, 2.42 eV, 3.15 eV, respectively. The E_{CBM} (or LUMO) can then be determined by adding up their bandgap: E_{CBM} (or LUMO) = -3.39 eV, -3.27 eV and -2.57, respectively. The calculated energy levels of GaN and PDA are close to the ones reported.⁶⁻⁹

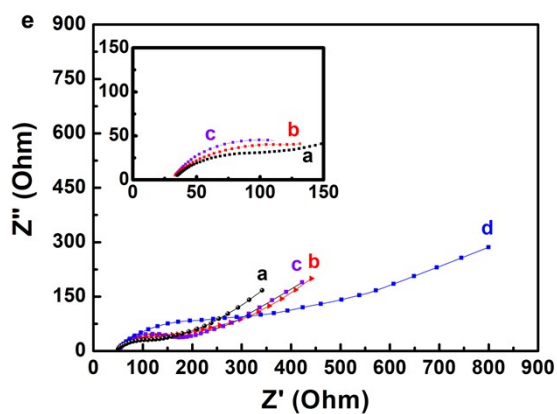
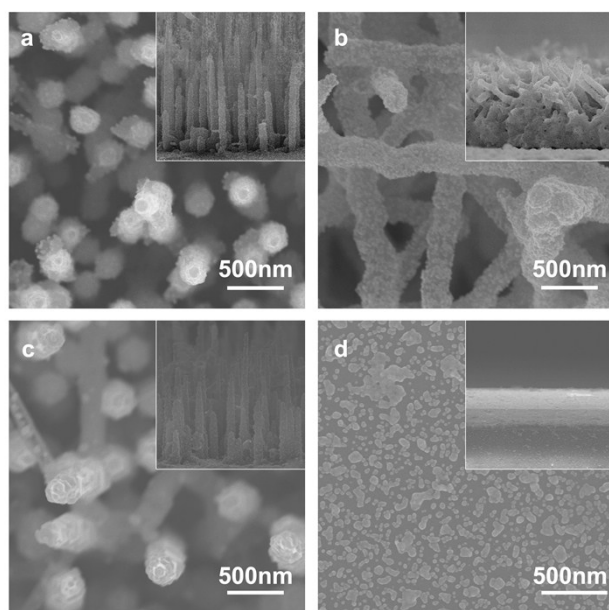


Figure S5 Plan view SEM images for (a) GaN nanowires array/PDA/Au NPs, (b) GaN nanowires/PDA/Au NPs, (c) GaN film/PDA/Au NPs and (d) GaN nanowires array/Au NPs. Insets show cross sectional SEM images for each electrode. All the electrodes are modified under identical conditions. (e) Electrochemical impedance spectra for the corresponding electrodes in (a)-(d), inset is the magnified EIS at the range of 0-200 Ohm.

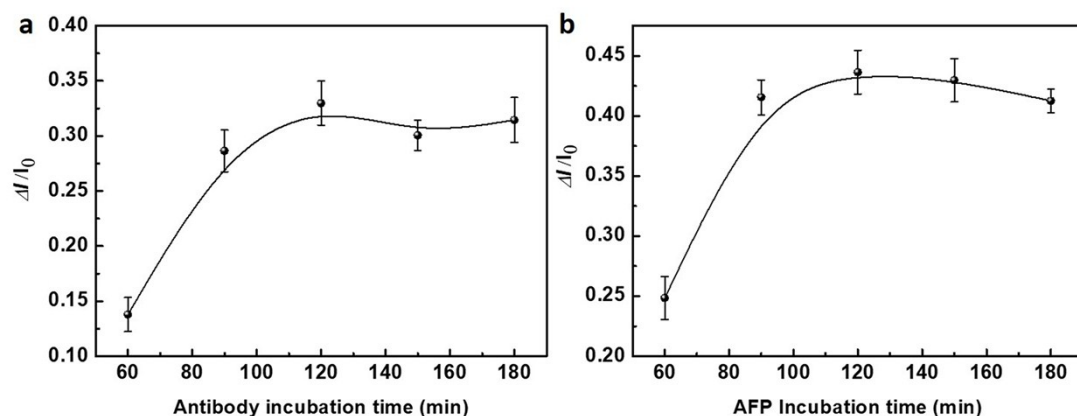


Figure S6 Effect of (a) anti-AFP antibody and (b) AFP antigen incubation time on the analytical performances of GaN nanowires array/PDA/Au NPs immunosensor.

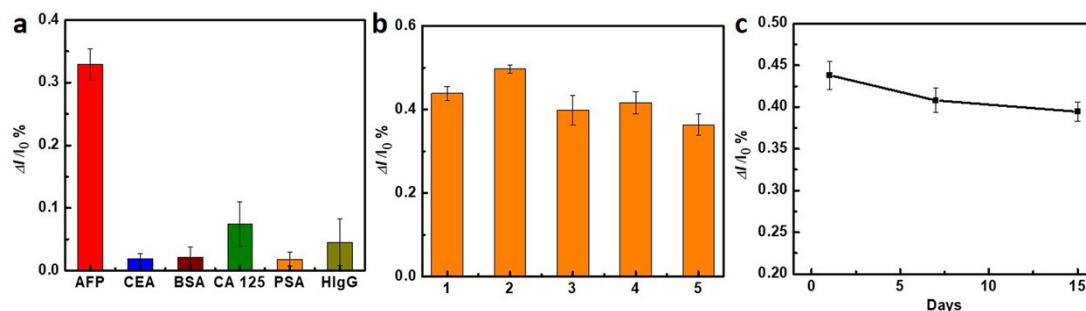


Figure S7 (a) Selectivity detection of immunosensors by incubating with AFP (0.1 ng/ml), CEA (10 ng/ml), HlgG (10 ng/ml), BSA (10 ng/ml) and CA 125 (1000U/ml), separately. (b) Repeatability test by detecting five groups of immunosensors incubated with 1 ng/ml AFP treated under identical conditions. (c) Stability of the immunosensor after storage at 4°C for 1 day, 7 days and 15 days, AFP concentration is 1 ng/ml.

Supplementary Tables

Table S1 Parameters obtained from the data fitting to the equivalent circuit shown in Figure 3b (All parameters are fitted by Zview software)

Parameters(Ω)	Curve a	Curve b	Curve c
R_s	50.15	51.93	50.98
CPE-T	5.299E-5	5.1705E-5	5.1952E-5
CPE-P	0.64671	0.65603	0.69452
Z_w -R	2995	12393	21626
Z_w -T	31.45	8662	529910
Z_w -P	0.45	0.34163	0.32032
R_{et}	448.2	188.2	96.04

Table S2 Recovery experiments for AFP detection in diluted human serum samples

SAMPLE	Added of AFP(ng/ml)	Found (ng/ml)	Recovery (%)	RSD/(n=5)
1	0.10	0.098	98.42%	3.5
2	1.00	1.057	105.70%	5.0
3	10.00	10.55	105.5%	4.5

Table S3 Concentration of AFP in human serum for several common neoplasms¹⁰

Clinical category	Number of patients	Number of AFP positive	Range of AFP (ng/ml)
Normal adults	50	0	<20
Hepatomas	19	18	160-5,500,000
Embryonal carcinomas of testes	6	5	1100-130,000
Viral hepatitis	11	6	24-87

References

1. J. Liu, Y. Liu, N. Y. Liu, Y. Z. Han, X. Zhang, H. Huang, Y. Lifshitz, S. T. Lee, J. Zhong and Z. H. Kang, *Science*, 2015, 347, 970-974.
2. J. H. Seo, R. Yang, J. Z. Brzezinski, B. Walker, G. C. Bazan and T.-Q. Nguyen, *Adv. Mater.*, 2009, 21, 1006-1011.
3. J. L. Lyons, A. Janotti and C. G. Van de Walle, *Physical Review B*, 2014, 89.
4. J. Tauc, R. Grigorovici and A. Vancu, *phys. stat. sol.*, 1966, 15, 627-637.
5. S. Chandra, P. Patra, S. H. Pathan, S. Roy, S. Mitra, A. Layek, R. Bhar, P. Pramanik and A.

- Goswami, *Journal of Materials Chemistry B*, 2013, 1, 2375-2382.
6. H. J. Nam, B. Kim, M. J. Ko, M. Jin, J. M. Kim and D. Y. Jung, *Chemistry*, 2012, 18, 14000-14007.
 7. S. Kim, G. H. Moon, G. Kim, U. Kang, H. Park and W. Choi, *J. Catal.*, 2017, 346, 92-100.
 8. M. Mishra, T. C. S. Krishna, N. Aggarwal and G. Gupta, *Appl. Surf. Sci.*, 2015, 345, 440-447.
 9. Z. F. Zhang, Q. K. Qian, B. K. Li and K. J. Chen, *ACS Appl. Mater. Interfaces*, 2018, 10, 17419-17426.
 10. P. G. Hulbert K. B. Silver, Stephen Feder, Samuel O. Freedman, and Joseph Shuster, *Proc. Natl. Acad. Sci. U. S. A.*, 1973, 70 526-530.